A high voltage silicon-on-insulator lateral insulated gate bipolar transistor with a reduced cell-pitch*

Luo Xiao-Rong(罗小蓉)†, Wang Qi(王 琦), Yao Guo-Liang(姚国亮), Wang Yuan-Gang(王元刚), Lei Tian-Fei(雷天飞), Wang Pei(王 沛), Jiang Yong-Heng(蒋永恒), Zhou Kun(周 坤), and Zhang Bo(张 波)

State Key Laboratory of Electronic Thin Films and Integrated Devices, University of Electronic Science and Technology of China, Chengdu 610054, *China*

(Received 31 May 2012; revised manuscript received 9 July 2012)

A high voltage (> 600 V) integrable silicon-on-insulator (SOI) trench-type lateral insulated gate bipolar transistor (LIGBT) with a reduced cell-pitch is proposed. The LIGBT features multiple trenches (MTs): two oxide trenches in the drift region and a trench gate extended to the buried oxide (BOX). Firstly, the oxide trenches enhance electric field strength because of the lower permittivity of oxide than that of Si. Secondly, oxide trenches bring in multi-directional depletion, leading to a reshaped electric field distribution and an enhanced reduced-surface electric-field (RESURF) effect. Both increase the breakdown voltage (BV). Thirdly, oxide trenches fold the drift region around the oxide trenches, leading to a reduced cell-pitch. Finally, the oxide trenches enhance the conductivity modulation, resulting in a high electron/hole concentration in the drift region as well as a low forward voltage drop (V_{on}). The oxide trenches cause a low anode–cathode capacitance, which increases the switching speed and reduces the turn-off energy loss (E_{off}). The MT SOI LIGBT exhibits a BV of 603 V at a small cell-pitch of 24 μm, a V_{on} of 1.03 V at 100 A/cm^{-2}, a turn-off time of 250 ns and E_{off} of 4.1×10^{-3} mJ. The trench gate extended to BOX synchronously acts as dielectric isolation between high voltage LIGBT and low voltage circuits, simplifying the fabrication processes.

Keywords: silicon-on-insulator, lateral insulated gate bipolar transistor, conductivity modulation, breakdown voltage, trench

PACS: 73.40.Ty, 73.61.Ng, 73.90.+f **DOI:** 10.1088/1674-1056/22/2/027303

1. Introduction

Insulated gate bipolar transistors (IGBTs) reduce drift region resistance by conductivity modulation and maintain a high breakdown voltage (BV).[1–3] The IGBT is thus one of the key devices for high voltage power integrated circuits (ICs) and has been widely used in electric vehicles and motor control. Furthermore, the lateral IGBT (LIGBT) is easily integrated with IC. However, there is a substrate-biased effect for LIGBTs based on bulk silicon. Silicon-on-insulator (SOI) has many advantages, such as high speed, superior isolation, and strong immunity to latch-up.[4–9] A dielectric trench in the drift region can reduce cell-pitch of power device.[10–14]

Combining the merits of the dielectric trench and SOI technologies, a new SOI LIGBT with multiple trenches (MT SOI LIGBT) is proposed. The SOI LIGBT is characterized by two oxide trenches in the drift region and one trench gate extended to the buried oxide (BOX). The two oxide trenches in the drift region have four merits for the MT SOI LIGBT: increasing the BV and switching speed, and reducing the cell-pitch and forward voltage drop (V_{on}). The extended trench gate reduces V_{on} and realizes the dielectric isolation between the high/low voltage regions in a high voltage IC.

2. Device structure and mechanism

The schematic cross section of the MT SOI LIGBT is shown in Fig. 1. The trench gate is located in the periphery of the new structure; two oxide trenches are placed in the drift region. W_t and D_t are the width and depth of the two oxide trenches, respectively. T_s and N_d are the thickness and doping concentration of the drift region, respectively. T_I is the thickness of the BOX.

There are two oxide trenches in the drift region so that a high lateral BV can be achieved. In the x direction, the Gauss law is expressed as

$$\varepsilon_{OX}E_{OX} = \varepsilon_{Si}E_{Si}, \tag{1}$$

where E_{Si} and E_{OX} are the electric field strengths of the Si and trench oxide at their interface, ε_{OX} and ε_{Si} are the relative permittivities of oxide and Si, respectively. The oxide trenches can sustain higher electric field strength than Si because of its lower permittivity.

The drift region is folded around the oxide trenches, resulting in a much smaller cell-pitch. Oxide trenches, the BOX,

*Projects supported by the National Natural Science Foundation of China (Grant No. 61176069), the State Key Laboratory of Electronic Thin Films and Integrated Devices, China (Grant No. CXJJ201004), and the National Key Laboratory of Analog Integrated Circuit, China (Grant No. 9140C090304110C0905).

†Corresponding author. E-mail: xrluo@uestc.edu.cn

© 2013 Chinese Physical Society and IOP Publishing Ltd

and the trench gate as insulator layers form several metal-insulator-semiconductor (MIS)-like structures. Figure 2 shows depletion boundary lines (dashed lines) and equi-potential contours at the different drain voltages, where arrows indicate the depletion directions in the drift region (e.g., "S" regions). Figure 2 demonstrates the multi-directional depletions caused by the MIS-like structures. The electric field distribution is well reshaped and $N_{\rm d}$ is greatly increased by the oxide trenches and the trench gate. According to the following equation in the drift region

$$\nabla \cdot E_{\rm Si} = \frac{q}{\varepsilon_{\rm s}} N_{\rm d}, \tag{2}$$

the high $N_{\rm d}$ leads to a high electric field strength $E_{\rm Si}$ in the drift region. In the y direction, the electric field strength in the BOX layer is thus enhanced according to $\varepsilon_{\rm OX} E_{\rm BOX} = \varepsilon_{\rm Si} E_{\rm S}$ in the SOI/BOX interface. The vertical BV is expressed as

$$BV_{\rm ver} = \alpha E_{\rm S} T_{\rm S} + E_{\rm BOX} T_{\rm I}, \tag{3}$$

where α ranges from 0.5 to 1.0, and $\alpha \approx 0.5$ in the one-dimensional approximation for the normal SOI device, $E_{\rm S}$ and $E_{\rm BOX}$ are the electric field strengths of Si and oxide in the SOI/BOX interface.

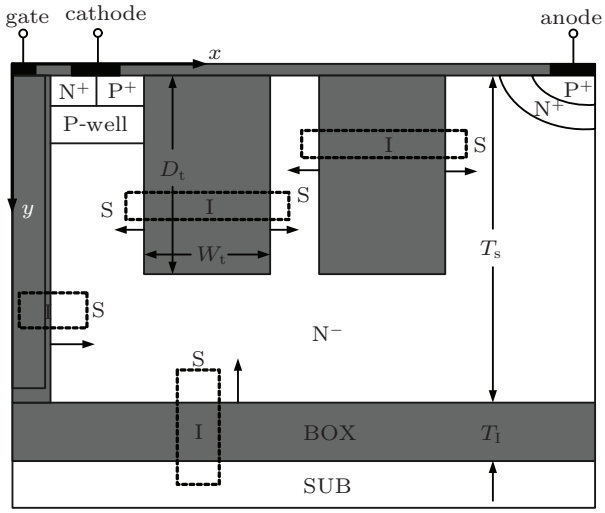


Fig. 1. Schematic cross section of the new MT SOI LIGBT.

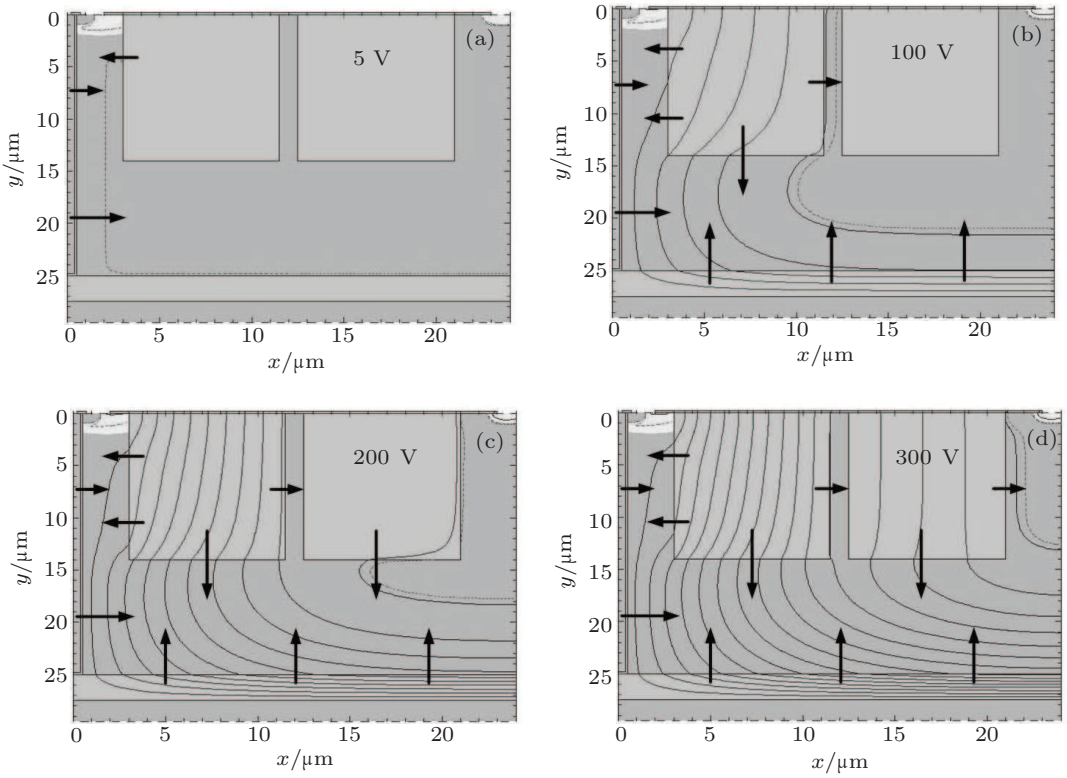


Fig. 2. Multi-directional depletions at (a) 5 V, (b) 100 V, (c) 200 V, and (d) 300 V.

Oxide trenches enhance the RESURF effect and thus increase the optimal $N_{\rm d}$. Furthermore, in the on-state, oxide trenches hinder the injected holes fast going into the p-body, which, thus, helps store the carriers in the drift region.[15] The extended trench gate widens the conduction area. All of the three factors (increased $N_{\rm d}$, enhanced carriers storage, and widened conduction area) contribute to a low forward voltage drop $V_{\rm on}$. A small anode–cathode capacitance is formed due to the oxide trenches with a low oxide permittivity. The smaller anode–cathode capacitance results in a higher switching speed

and a lower switching power loss E_{off}.

3. Results and discussion

Figure 3 shows the electric field distributions for the new MT SOI LIGHT, trench-gate SOI LIGBT (TG SOI LIGBT), and conventional SOI LIGBT (Con. SOI LIGBT). All three devices are optimized to gain the highest BV at the same device dimensional parameters. Low permittivity of oxide results in high field strength in the oxide trench as shown in Fig. 3(a). In the x direction, the surface electric field in the oxide trench of the MT SOI is much higher than those of the TG SOI and Con. SOI in the Si drift region. The average E-field strength in the oxide is over 30 V/μm for the MT SOI LIGBT, while the average E-field strength in the Si is about 10 V/μm for the TG SOI and Con. SOI. The two oxide trenches strengthen multi-directional depletion and reshape electric field distribution, resulting in an increased N_d and an enhanced RESURF effect. The electric field strength is enhanced in the SOI and BOX under the anode as well. Figure 3(b) shows electric field distributions in the y direction. The values of E_S at the SOI/BOX interface tremendously increase from 1.5 V/μm (Con. SOI) and 7.7 V/μm (TG SOI) to 26 V/μm (MT SOI), and the values of E-field (E_{BOX}) of the BOX increase from 35 V/μm (Con. SOI) and 23 V/μm (TG SOI) to 78 V/μm (MT SOI). The voltages sustained by both the SOI layer and BOX (called V_S and V_I) increase. Consequently, BV is obtained to be 603 V by simulation for the MT SOI LIGBT with a cell-pitch of 24 μm. The two-dimensional equi-potential contours in Fig. 4 demonstrate the reshaped electric field distributions in the x and y directions. In Fig. 4(c), the thick SOI layer greatly weakens the RESURF effect and the region in the dashed rectangle does not sustain the voltage drop, and the optimal N_d is 6.0×10^{13} cm^{-3}. However, there are inversion layer holes enhancing the E-field of the BOX, wherein the electric displacement continuity is written as $\varepsilon_{OX}E_{BOX} = \varepsilon_{Si}E_S + Q_H$ for the Con. SOI LIGBT, where Q_H is the interface charge density (C/cm^2). In Fig. 4(b), the extended trench gate as a field plate improves the E-field distribution in the Si drift region, the BV increases up to 183 V from 166 V of the Con. SOI LIGBT.

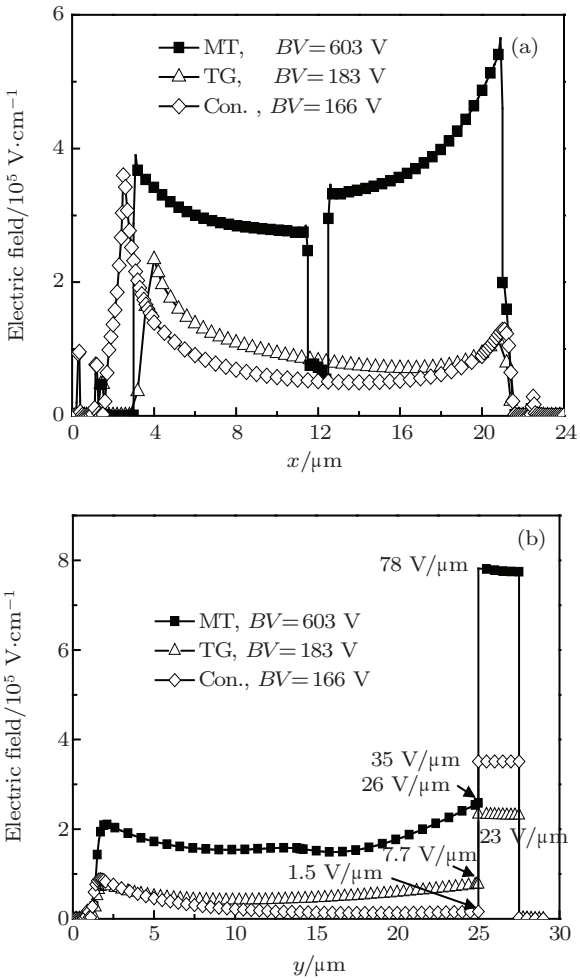


Fig. 3. (a) Lateral electric field distributions at surface, and (b) vertical electric field distributions under the anode region.

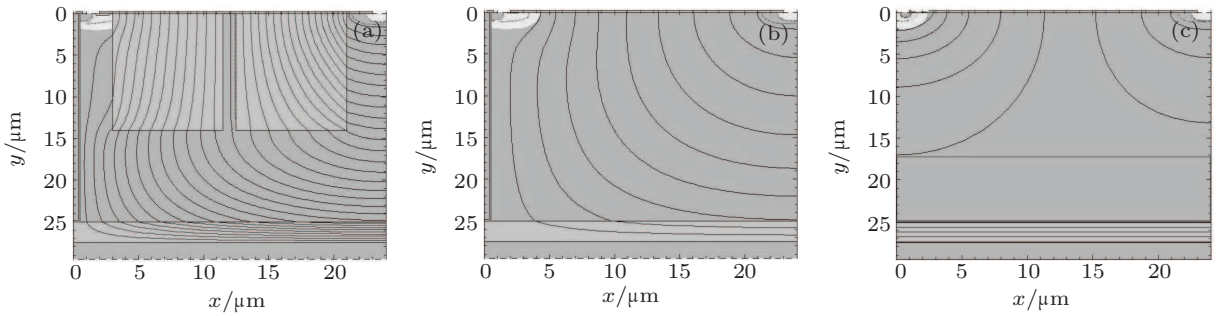


Fig. 4. Equi-potential contours (20 V/contour) for (a) new MT SOI LIGBT, (b) TG SOI LIGBT, and (c) Con. SOI LIGBT.

The influences of W_t and D_t on BV are discussed in Fig. 5(a). The wider the oxide trench, the higher the lateral breakdown voltage is. Consequently, BV increases as W_t increases. The high and deep oxide trenches (i.e., the large values of the W_t and D_t) enhance the RSURF effect, and therefore increase the E-field strengths in the Si and the BOX. Fig-

ure 5(b) shows the E-field distributions in the y direction. The BV increases from 548 V to 610 V with D_t increasing from 10 μm to 16 μm, in which V_S increases from 382 V to 413 V and V_I from 166 V to 197 V. For the 600-class LIGBT, we choose $D_t = 14$ μm and $W_t = 8.5$ μm considering the fabrication process.

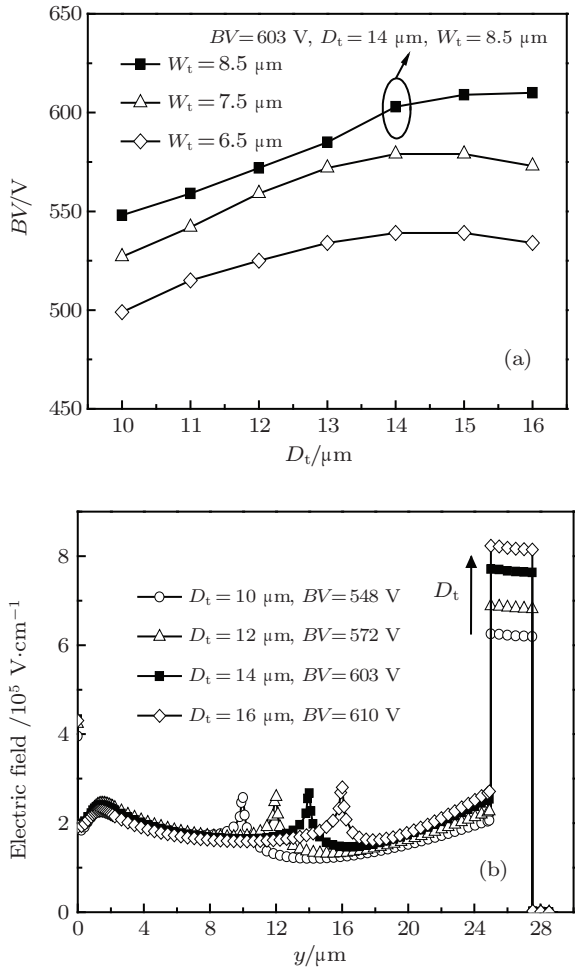


Fig. 5. (a) Influences of W_t and D_t on BV, and (b) vertical electric fields along the right side ($x = 21.01$ μm) of oxide trench for different values of D_t.

Figure 6 shows the dependence of the BV on cell-pitch (or W_t). It indicates that the BV increases when the cell-pitch increases with W_t increasing, with other parameters unchanged. At a 28-μm cell-pitch, BV reaches a saturated value of 630 V due to vertical breakdown voltage as shown in Eq. (3), where T_S and T_I remain constant. For the new MT SOI LIGBT structure, a high BV over 600 V is achieved with a reduced cell-pitch of 24 μm.

Figure 7(a) shows the values of V_{on} for three devices in this paper, and V_{on} is the forward voltage drop at the current density of 100 A/cm^2. The values of V_{on} of the MT, TG, and conventional SOI LIGBTs are 1.03 V, 1.11 V, and 1.31 V, respectively. Three factors contribute to a low V_{on}: the high electron and hole concentration; the high optimal N_d; and the widened conduction due to the extended trench gate. Figure 7(b) shows the electron/hole concentrations in the drift regions in the on-state. The MT SOI LIGBT has the highest electron/hole concentration because the oxide trench helps store the carriers, and the difference between electron concentration and hole concentration is the N_d in Fig. 7(b).

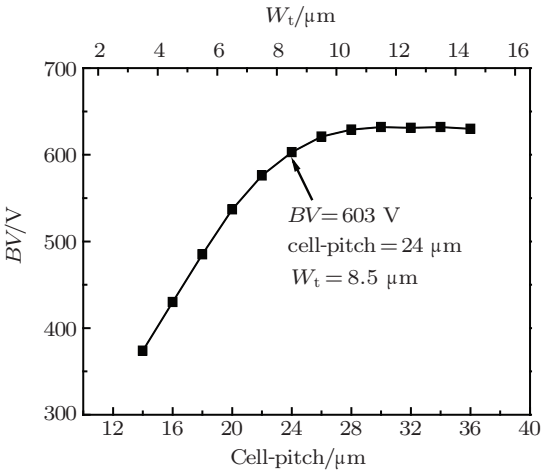


Fig. 6. BV of MT SOI LIGBT versus cell-pitch (or W_t).

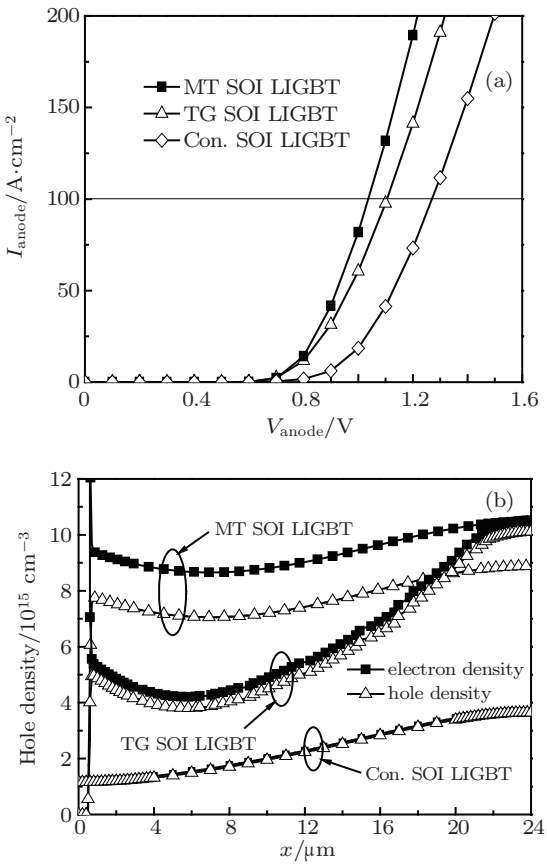


Fig. 7. Curves of I_{anode} versus V_{anode} (a) and hole/electron density at 100 A/cm^2 versus x (b) for three devices.

A smaller anode–cathode capacitance forms in the drift region due to the lower permittivity of the trench oxide, resulting in a high switching speed. As shown in Fig. 8, the turn-off

time of the MT SOI LIGBT is significantly reduced to 250 ns compared with 450 ns of the TG SOI LIGBT and 600 ns of the Con. SOI LIGBT. Consequently, a small E_{off} of 4.1×10^{-3} mJ is gained compared with 9.2×10^{-3} mJ of the TG SOI LIGBT and 11.6×10^{-3} mJ of the Con. SOI LIGBT.

Table 1 shows the optimized results for the three structures. The structure of the MT SOI LIGBT shows a high performance in the sense of BV, V_{on}, turn-off time, and E_{off} compared with the other two structures. Turn-off time of the TG SOI LIGBT is shorter than that of the Con. SOI LIGBT, which is because the large field plate performed by the trench gate can enhance the hole extraction during turn-off.

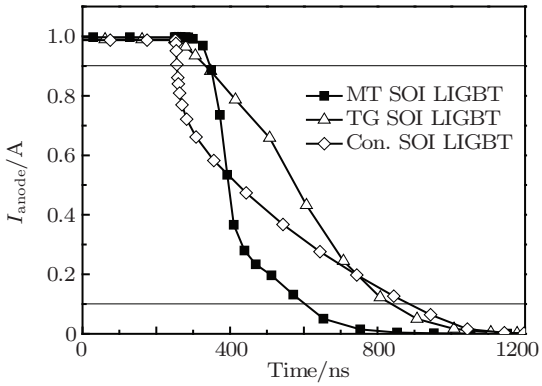


Fig. 8. Curves of turn-off current I_{anode} versus time for MT SOI LIGBT, TG SOI LIGBT, and Con. SOI LIGBT.

Table 1. Parameters BV, V_{on}, N_d, turn-off time, E_{off} for MT, TG, Con. SOI LIGBT with same cell-pitch.

Cell-pitch/24 μm	BV/V	V_{on}/V	N_d/cm^{-3}	Turn-off time/ns	E_{off}/mJ
MT SOI LIGBT	603	1.03	1.7×10^{15}	250	4.1×10^{-3}
TG SOI LIGBT	183	1.11	4.0×10^{14}	450	9.2×10^{-3}
Con. SOI LIGBT	166	1.31	6.0×10^{13}	600	11.6×10^{-3}

4. Conclusion

A trench-gate SOI LIGBT with two oxide trenches in the drift region is proposed and investigated by simulation. The oxide trenches enhance the electric field strength due to the lower permittivities of oxide and reshaped electric field distribution, resulting in a high BV. The oxide trenches help store the carriers and thus reduce the forward voltage drop. The oxide trenches reduce the cell-pitch and the turn-off time and power loss. Compared with the Con. SOI LIGBT, the MT SOI LIGBT increases the BV by 263% and reduces the V_{on} by 21%. The turn-off time and E_{off} are reduced by 58% and 65% compared with those of the Con. SOI LIGBT, respectively. The trench gate extended synchronously realizes the dielectric isolation between high/low voltage regions, thereby simplifying the fabrication processes.

References

[1] Baliga B J and Alder M S 1982 *Electron Devices Meeting*, December 13–15, 1982, San Francisco, USA, **26** 264

[2] Motto E R and Donlon J F 2004 *APEC*, February 22–26, 2004, Anaheim, USA, p. 235

[3] Jeong H and Fossum J G 1988 *Bipolar Circuits and Echnology Meeting*, September 12–13, 1988, Minneapolis, USA, p. 107

[4] Luo X R, Zhang B and Li Z J 2007 *Solid-State Electron.* **51** 493

[5] Luo X R, Li Z J, Zhang B and Fu D P 2008 *IEEE Electron. Dev. Lett.* **29** 1395

[6] Luo X R, Zhang B and Li Z J 2007 *IEEE Electron. Dev. Lett.* **28** 422

[7] Luo X R, Wang Y G, Deng H and Udrea F 2010 *Chin. Phys.* B **19** 077306

[8] Hu S D, Li Z J and Zhang B 2009 *Chin. Phys.* B **18** 315

[9] Hu S D, Li Z J, Zhang B and Luo X R 2010 *Chin. Phys.* B **19** 037303

[10] Son W S, Sohn Y H and Choi S 2004 *Microelectron. J.* **35** 393

[11] Fujishima N and Salama C 1997 *IEDM*, December 10–13, 1997, Washington, USA, p. 359

[12] Fujishima N, Sugi A and Salama C 2006 *US Patent* 7005352

[13] Varadarajan K R, Chow T P and Wang J 2007 *Proc. IEEE ISPSD* 2007 233

[14] Johnny K, Sin O and Wan C 1993 *US Patent* 5227653

[15] Kang X, Lu L, Wang X, Santi E, Hudgins J L, Palmer P R and Donlon J F 2003 *Industry Applications Conference*, October 12–16, Salt Lake City, USA, p. 892